Journal of Animal Science, 2023, **101**, 1–12
https://doi.org/10.1093/jas/skad271
Advance access publication 10 August 2023
Animal Genetics and Genomics

Exon–intron split analysis reveals posttranscriptional regulatory signals induced by high and low n-6/n-3 polyunsaturated fatty acid ratio diets in piglets

Yron Joseph Yabut Manaig,[†,‡,‖,1,2] Emilio Mármol-Sánchez,[$,¶,1] Anna Castelló,[†,‡] Anna Esteve-Codina,[**] Silvia Sandrini,[‖] Giovanni Savoini,[‖] Alessandro Agazzi,[‖] Armand Sánchez,[†,‡] and Josep M. Folch[†,‡]

[†]Departament de Ciència Animal i dels Aliments, Universitat Autònoma de Barcelona, Barcelona 08193, Spain
[‡]Plant and Animal Genomics, Centre for Research in Agricultural Genomics (CRAG), CSIC-IRTA-UAB-UB, Campus Universitat Autònoma de Barcelona, Barcelona 08193, Spain
[‖]Department of Veterinary Medicine and Animal Sciences, Università degli Studi di Milano, Lodi 26900, Italy
[$]Science for Life Laboratory, Department of Molecular Biosciences, The Wenner-Gren Institute, Stockholm University, Stockholm 11418, Sweden
[¶]Centre for Palaeogenetics, Stockholm 10691, Sweden
[**]Functional Genomics, CNAG-CRG, Centre for Genomic Regulation (CRG), Barcelona Institute of Science and Technology (BIST), Barcelona 08028, Spain

[1]These authors contributed equally to this work.
[2]Corresponding author: yronjosephmanaig@gmail.com

Abstract

Polyunsaturated fatty acids (**PUFA**), such as omega-6 (n-6) and omega-3 (n-3), play a vital role in nutrient metabolism, inflammatory response, and gene regulation. microRNAs (**miRNA**), which can potentially degrade targeted messenger RNAs (**mRNA**) and/or inhibit their translation, might play a relevant role in PUFA-related changes in gene expression. Although differential expression analyses can provide a comprehensive picture of gene expression variation, they are unable to disentangle when in the mRNA life cycle the regulation of expression is taking place, including any putative functional miRNA-driven repression. To capture this, we used an exon–intron split analysis (**EISA**) approach to account for posttranscriptional changes in response to extreme values of n-6/n-3 PUFA ratio. *Longissimus dorsi* muscle samples of male and female piglets from sows fed with n-6/n-3 PUFA ratio of 13:1 (**SOY**) or 4:1 (**LIN**), were analyzed in a bidirectional contrast (LIN vs. SOY, SOY vs. LIN). Our results allowed the identification of genes showing strong posttranscriptional downregulation signals putatively targeted by significantly upregulated miRNA. Moreover, we identified genes primarily involved in the regulation of lipid-related metabolism and immune response, which may be associated with the pro- and anti-inflammatory functions of the n-6 and n-3 PUFA, respectively. EISA allowed us to uncover regulatory networks complementing canonical differential expression analyses, thus providing a more comprehensive view of muscle metabolic changes in response to PUFA concentration.

Lay Summary

The relationship between dietary lipids, such as omega-6 and omega-3 polyunsaturated fatty acids (**PUFA**), and gene expression regulation was explored in piglet muscle. While these PUFA can influence nutrient metabolism and inflammatory response, small regulatory molecules called microRNAs (**miRNA**) can also influence the activity of genes. In this experiment, we used a computational approach dubbed exon–intron split analysis (**EISA**) to fully understand the role of miRNA in this context and how the genes and miRNA respond to changes in PUFA levels. Our findings demonstrated that some genes involved in lipid metabolism and immune response were affected by different PUFA concentrations and that EISA provides a more comprehensive view of how genes are regulated throughout their life cycle.

Keywords: Exon–intron split analysis, microRNA, messenger RNA, piglets, PUFA

Abbreviations: AA, arachidonic acid; ALA, alpha-linolenic acid; bp, base pair; DE, differential expression; DGLA, dihomo-gamma-linoleic acid;EISA, exon–intron split analysis; EPA, eicosapentaenoic acid; ETA, eicosatrienoic acid; FC, fold-change; GLA, gamma-linoleic acid; GO, Gene Ontology; LA, linoleic acid; LD, *longissimus dorsi*; LIN, diet with n-6/n-3 PUFA ratio of 4:1; LIN-F, female piglets from sows fed with diet with n-6/n-3 PUFA ratio of 4:1; LIN-M, male piglets from sows fed with diet with n-6/n-3 PUFA ratio of 4:1; miRNA, microRNAs; mRNA, messenger RNA; n-6, omega-6; n-3, omega-3; n-6/n-3, omega-6/omega-3 PUFA ratio; nts, nucleotides; pre-mRNA, unprocessed messenger RNA; PTc, posttranscriptional change; PUFA, polyunsaturated fatty acid; *r*, Pearson's pairwise correlation coefficient; *rex*, Pearson's pairwise correlation coefficient of exonic counts; *rint*, Pearson's pairwise correlation coefficient of intronic counts; RIN, RNA integrity number; RNA, ribonucleic acid; RNA-Seq, RNA sequencing; SOY, diet with n-6/n-3 PUFA ratio of13:1; SOY-F, female piglets from sows fed with diet with n-6/n-3 PUFA ratio of 13:1; SOY-M, male piglets from sows fed with diet with n-6/n-3 PUFA ratio of 13:1; UTR, untranslated region; ΔEx, change in exonic counts; ΔInt, change in intronic counts; Δr, difference from exonic and intronic correlation values; 7mer-1A, exact match to positions 2-7 of the mature miRNA followed by an "A"; 7mer-m8, exact match to positions 2-8 of the mature miRNA; 8mer, exact match to positions 2-8 of the mature miRNA followed by an "A"

Received May 6, 2023 Accepted August 8, 2023.

Introduction

The landscape of posttranscriptional regulation of gene expression has been expanded significantly since the discovery of microRNAs (**miRNA**), a class of regulatory small noncoding ribonucleic acid (**RNA**) molecules of ~22 nucleotides in length (Bartel, 2018). miRNA have the ability to fine-tune the expression of genes linked to a specific metabolic pathway by base-pairing to the 3′ untranslated region (3′ **UTR**) of target messenger RNAs (**mRNA**), eliciting their degradation and/or inhibiting their translation. This could potentially alter the translation of tens or hundreds of different mRNA transcripts into functional proteins (Filipowicz et al., 2008; Naeli, Winter et al., 2022). High-throughput transcriptome sequencing (**RNA-Seq**) has emerged as one of the primary methods in providing significant amount of data regarding gene expression profiles among multiple species, including pigs, and across diverse biological conditions (Ramayo-Caldas et al., 2012; Horodyska et al., 2018; Xing et al., 2021). One of the most popular applications of RNA-Seq data is differential expression (**DE**) analysis. This method enables the identification of genes that have different average expression levels between two or more conditions, which may aid to further explain some key phenotypic variations observed (Frazee et al., 2014; Costa-Silva et al., 2017; McDermaid et al., 2019). Although extremely helpful, utilizing DE analysis to infer gene regulation has a significant drawback: it does not account for transcriptional or posttranscriptional regulation that might alter gene expression estimates (Mármol-Sánchez et al., 2022).

To circumvent this limitation, Gaidatzis et al. (2015) developed the exon–intron split analysis (**EISA**) to disentangle the transcriptional and posttranscriptional components of gene regulation by measuring the changes between the exonic and intronic reads from expressed mRNA transcripts. The EISA approach considers the presence of reads mapping to intronic regions as being mainly derived from unprocessed mRNAs (**pre-mRNA**) before splicing, hence indicative of transient transcriptional activation/repression in the nucleus. For modeling the posttranscriptional component of gene expression, EISA takes the difference between exonic and intronic changes, thus integrating the intronic fraction as an event happening before any posttranscriptional modification that occurs in the cytoplasm (Gaidatzis et al., 2015). Using the posttranscriptional signals determined by EISA and expression changes at the miRNA level, we can integrate both layers of information to link differentially expressed miRNA and their targeted mRNA at the posttranscriptional level.

Polyunsaturated fatty acids (**PUFA**), particularly the omega-6 (n-6) and omega-3 (n-3) series, have the ability to influence and control gene expression and transcription factor activity, thus potentially affecting nutrient metabolism, regulatory networks, signal-transduction pathways, mRNA transcription, splicing, and protein synthesis (Ntambi and Bené, 2001; Georgiadi and Kersten, 2012; Manaig et al., 2023). Metabolites derived from n-6 and n-3 PUFA are common precursors of eicosanoids that can regulate inflammation. As such, these two are also antagonistic in their inflammatory nature, with n-6 PUFA acting as pro-inflammatory and n-3 PUFA as anti-inflammatory modulators, respectively (Zivkovic et al., 2011; Sakayori et al., 2020). In livestock, maintaining a low ratio between n-6 and n-3 PUFA on feeding diets has shown beneficial effects on reproductive and productive performance for both sows and piglets (Nguyen et al., 2020; Manaig et al., 2022).

To better understand the combined effects of posttranscriptional regulation and PUFA on mRNA expression, as well as the miRNA regulatory contribution on porcine *longissimus dorsi* (**LD**) muscle, we determined posttranscriptional signals using EISA on male and female piglets from sows fed high and low n-6/n-3 PUFA ratio diets. Moreover, we correlated both mRNA and miRNA expression values to the PUFA profile of skeletal muscle tissue.

Materials and Methods

Ethical statement

All experimental protocols were approved by the ethical committee of the University of Milan (OPBA 22/2020), in pursuant to Article 1 paragraphs 1 and 2 of Rectoral Decree no. 0296049 of 20/07/2015 and Regolamento Dell'Organismo Preposto Al Benessere Degli Animali.

Experimental design and animal material

Twenty-three suckling piglets were obtained from a pool of piglets nourished only with both sow's colostrum and milk. A detailed description of the experimental design adopted was as previously reported by Manaig et al. (2022). Briefly, the gestating and lactating sows were divided between two treatments and fed ad libitum with diets containing n-6/n-3 PUFA ratios of 4:1 (**LIN**) or 13:1 (**SOY**). Such ratios were attained through the addition of soybean oil (n-6) or linseed oil (n-3) to the basal diet and maintained throughout the whole experimental period. At the end of lactation—average 25.75 d of lactation—and before weaning, LD skeletal muscle samples were collected from selected piglets immediately after slaughter, snapped-frozen, and stored at −80 °C until use. Fatty acids profiling of LD muscles was done using gas chromatography with a flame ionization detector. A list of the measured fatty acids in the current study is available in Supplementary Table S1a. The selection of the 23 piglets included in this study was based on the analyzed values of n-6/n-3 PUFA ratio for each treatment diet, i.e., 12 (LIN; 6 males, 6 females) and 11 (SOY; 6 males, 5 females) piglets were kept for further analyses. One female piglet from SOY diet was discarded due to unexpected values in PUFA profiling. Recorded phenotypic values from the selected piglets are summarized in Supplementary Table S1b.

RNA extraction, library preparation, and sequencing

Approximately 90 mg of LD tissue per sample was disrupted and homogenized in 700 µL of QIAzol Lysis Reagent (QIAGEN, Germantown, ML, USA) using 2 mL Lysing matrix D tubes (MP Biomedicals, Santa Ana, CA) and a Precellys 24 instrument (Bertin Technologies, Rockville, MD). The miRNeasy Kit (QIAGEN, Germantown) was used to extract the total RNA fraction while keeping small RNA molecules as per manufacturer's specifications. RNA was then eluted with 30 µL of ultrapure water. RNA concentration and purity were determined with a Nanodrop ND-1000 spectrophotometer (Thermo Fisher Scientific, Barcelona, Spain). RNA integrity was assessed with a Bioanalyzer-2100 equipment (Agilent Technologies Inc., Santa Clara, CA, USA), using the Agilent RNA 6000 Nano Kit (Agilent Technologies Inc.) and allowing an RNA integrity number (**RIN**) ≥ 7. Sequencing

libraries were prepared with the TruSeq SBS Kit v3-HS (Illumina Inc., CA, USA). A minimum of 30 million hits of 75 bp-length paired-end reads and a minimum of 10 million hits of 50 bp-length single-end reads were acquired per sample for mRNA and small RNAs, respectively, using an Illumina HiSeq 3000/4000 equipment (CNAG-CRG, Barcelona, Centro Nacional de Análisis Genómico; https://www.cnag.cat/).

RNA-Seq and small RNA-Seq data processing

The FastQC (Andrews, 2010) tool was used to perform quality control on raw fastq files from RNA-Seq and small RNA-Seq sequences. Illumina adapters were trimmed using the Cutadapt v3.2 (Martin, 2011) software. Only reads with 18 to 25 nucleotides (**nts**) in length after adapter trimming (compatible with the expected length of mature miRNA transcripts) were kept from small RNA-Seq data. Sequences from RNA-Seq data were mapped with HISAT2 (Kim et al., 2019) aligner using default parameters, while small RNA-Seq data alignment was performed with the Bowtie v1.2.1.1 (Langmead et al., 2009) tool, allowing no mismatches in the local mapping and a maximum of 20 multimapping spots per read, while reporting the best hit among the stacked multiple mappings (*bowtie-n 0-m 20-k 1-best*) (Mármol-Sánchez et al., 2020). Both RNA-Seq and small RNA-Seq alignments were done against the reference pig genome Sscrofa11.1 (Warr et al., 2020). Dedicated annotations of exonic and intronic regions across the pig genome, excluding exonic–intronic site overlaps (10 bp at both ends of introns), were generated from all the annotated genes in the Sscrofa11.1 porcine reference assembly (Ensembl v.106) by using the *makeEISAgtfs* function from the EISAcompR pipeline (https://github.com/emarmolsanchez/EISAcompR) (Mármol-Sánchez et al., 2022). Mature miRNA and mRNA expression levels, including the independent expression levels for exons and introns, were quantified using the featureCounts v2.0.3 software (Liao et al., 2014).

Differential expression analyses

Differential expression analyses were carried out by using the exonic counts of mRNA and the mature miRNA expression levels. We only considered genes with an average expression value above 1 count per million in at least 50% of samples within each treatment group and sex classification—LIN male (**LIN-M**), LIN female (**LIN-F**), SOY male (**SOY-M**), and SOY female (**SOY-F**). Gene expression differences were tested separately for each sex, i.e., we compared male piglets fed with LIN diet (LIN-M) against male piglets fed with SOY diet (SOY-M), as well as female piglets fed with LIN diet (LIN-F) against female piglets fed with SOY diet (SOY-M). Raw counts were normalized for library size homogenization with the trimmed mean of M-values method (Robinson and Oshlack, 2010) and the statistical significance of average expression differences between groups was assessed with a quasi-likelihood *F*-test using edgeR software (Robinson et al., 2010), and including a batch covariate in the regression model (Supplementary Table S1b). Multiple testing correction was performed with the false discovery rate approach (Benjamini and Hochberg, 1995). mRNA and mature miRNA from DE analyses were considered significant at an absolute fold-change (**FC**) > 1.5 and q-value < 0.05. Suckling piglets from LIN diet (LIN-M and LIN-F) were defined as reference controls, meaning that any given gene upregulation (i.e., mRNA or miRNA) would imply an overexpression in SOY-fed piglets (SOY-M and SOY-F) with respect to LIN-fed piglets, leading to a positive fold change, and vice versa.

Exon–intron split analysis

Posttranscriptional changes in messenger RNAs between diets were inferred using the EISAcompR pipeline (https://github.com/emarmolsanchez/EISAcompR) (Mármol-Sánchez et al., 2022).

We only evaluated genes with both exonic and intronic read counts successfully quantified. The increase of intronic and exonic counts in LIN-M vs. SOY-M or LIN-F vs. SOY-F and, conversely, in SOY-M vs. LIN-M, represented the detected variations for every *i*th gene. The increase in both the exonic and intronic fractions was calculated as follows: $\Delta\text{Int} = \text{Int}_{2i} - \text{Int}_{1i}$ for intronic counts; and $\Delta\text{Ex} = \text{Ex}_{2i} - \text{Ex}_{1i}$ for exonic counts, where Int_2 and Ex_2 represent each average *i*th gene expression in the SOY diet for LIN vs. SOY, or the average *i*th gene expression in the LIN diet for SOY vs. LIN, respectively. We then estimated the levels of posttranscriptional change (**PTc**) in mRNA expression. In this way, the difference between ΔEx and ΔInt represents the PTc component (PTc = ΔEx − ΔInt) (Pillman et al., 2019). The top 5% of expressed genes with the most negative PTc scores were selected as genes displaying strong posttranscriptional regulatory signals. We also narrowed down our filtering criteria to those genes that had strongly reduced ΔEx showing at least 1.5-fold downregulation (i.e., $\Delta\text{Ex} < -0.58$ in the $\log_2$ scale).

miRNA target prediction

Canonical target site prediction of the binding of miRNA seeds (second to eighth 5′ nucleotide position in the mature miRNA) to the 3′ UTR of target mRNA genes was performed by making use of the seedVicious v1.1 tool (Marco, 2018). The annotated 3′ UTRs from porcine mRNA were retrieved from the Biomart database (https://www.ensembl.org/info/data/biomart/index.html, Sscrofa11.1 v106), while mature porcine miRNA sequences were obtained from miRBase v22.1 (Kozomara et al., 2019). Only those mRNAs among the top 5% of expressed genes with the most negative PTc scores and at least 1.5-fold exonic (ΔEx) downregulation, as well as significantly upregulated miRNA, were selected as input. miRNA-mRNA interactions of type 8mer, 7mer-m8, and 7mer-A1 were considered (Bartel, 2018).

Gene ontology and pathway enrichment analysis

Differentially expressed mRNA from exonic counts and those expressed genes with the top 5% most negative PTc scores and ΔEx repression of at least 1.5-fold among LIN-M vs. SOY-M, SOY-M vs. LIN-M, and LIN-F vs. SOY-F contrasts were subjected to Gene ontology (**GO**) and pathway enrichment analyses. This was performed using Cytoscape v3.7.1 software with the ClueGO v2.5.4 plug-in application to determine enriched Biological Process terms (Shannon et al., 2003; Bindea et al., 2009). Identification of enriched terms was done using a two-sided hypergeometric test of significance with a false discovery rate approach for multiple testing correction (Benjamini and Hochberg, 1995).

Correlation between mRNA, miRNA, and fatty acids profile of LD muscle

We estimated the Pearson's pairwise correlation coefficients (r) between genes within the top 5% with the most negative

PTc scores and at least 1.5-fold reduction in ΔEx values that were putatively targeted by significantly upregulated miRNA and the set of significantly upregulated miRNA. Exonic and intronic normalized $\log_2$ counts for mRNAs, separately, and mature miRNA normalized $\log_2$ counts were used. Additionally, we correlated the percent concentration of analyzed PUFA values of porcine LD muscle, as previously reported by Manaig et al. (2022) with exonic normalized $\log_2$ counts for mRNAs, and with mature miRNA normalized $\log_2$ counts, respectively. Pearson's pairwise correlation coefficients (r) and their significance were computed with the *corr.test* R function. Multiple testing correction was performed with the false discovery rate approach (Benjamini and Hochberg, 1995).

Results

Evaluation of posttranscriptional signals in LD muscle from male piglets

Differential expression and EISA

RNA-Seq data for male piglets resulted in around 105 million reads per sample. From these, ~100 million reads (95%) per sample were successfully mapped to the Sscrofa11.1 reference assembly. Around 9 million reads per sample were kept from small RNA-Seq data after length filtering (18 to 25 nts), from which ~5.8 million reads (65%) were successfully mapped to the Sscrofa11.1 reference assembly, and ~75% of them were assigned to the 415 annotated porcine miRNA loci considered. The porcine reference assembly was then divided into its exonic and intronic regions to allow a split quantification of mapped reads from RNA-Seq data. Approximately 82% of the mapped reads from RNA-Seq were assigned to exonic regions, while only 4% of the mapped reads overlapped to intronic regions.

Using the edgeR software, we detected a total 11,055 porcine mRNA as sufficiently expressed, 222 of which were differentially expressed with an absolute FC value greater than 1.5 and a q-value less than 0.05 (Supplementary Table S2a). From these, 174 genes were upregulated and 48 were downregulated in SOY-M pigs with respect to LIN-M pigs, as illustrated in Figure 1. A full list of differentially expressed genes is available in Supplementary Table S2b. DE analyses on small RNA-Seq data highlighted a total of 62 significantly differentially expressed miRNA—29 downregulated and 33 upregulated miRNA in SOY-M piglets with respect to LIN-M piglets (Supplementary Table S3).

For the LIN-M vs. SOY-M contrast, EISA revealed 11 genes within the top 5% negative PTc scores with at least 1.5-fold ΔEx reduction as shown in Table 1. Three out of these 11 genes (27.27%) were also reported to be significantly downregulated (FC > −1.5; q-value < 0.05) in SOY-M piglets according to canonical differential expression analyses (Supplementary Table S2a).

On the other hand, reversing our contrast to SOY-M vs. LIN-M (SOY-M piglets are now considered as the reference group) allowed us to identify 97 mRNA within the top 5% negative PTc scores and at least 1.5-fold ΔEx reduction in LIN-M piglets (summarized in Supplementary Table 4). We also observed that out of these 97 genes, 22 (22.68%) of them were significantly downregulated (FC > −1.5; q-value < 0.05) in LIN-M piglets after canonical DE analyses (Supplementary Tables S2a and S4).

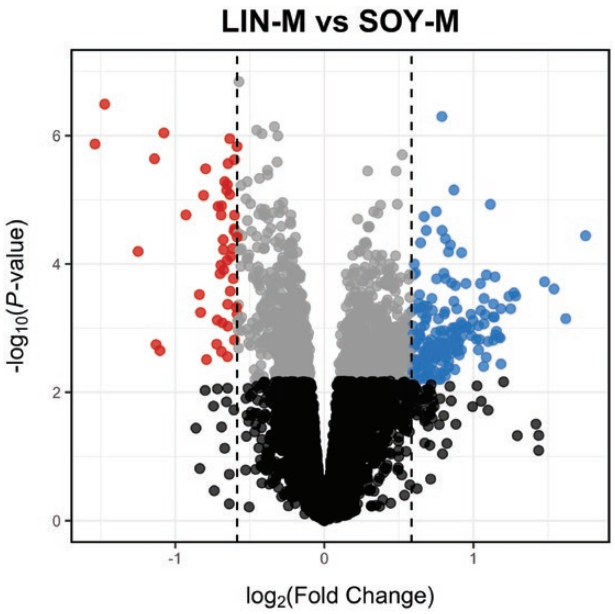

Figure 1. Volcano plot showing differentially expressed genes (|FC| > 1.5 and q-value < 0.05) in response to extreme n-6/n-3 PUFA ratio in *longissimus dorsi* skeletal muscle. Genes with P-value > 0.05 are depicted in black. Upregulated genes (blue) correspond to genes overexpressed in SOY-M with respect to LIN-M piglets while downregulated genes (red) are those repressed in SOY-M compared to LIN-M piglets.

Target prediction between mRNA with relevant PTc signals and upregulated miRNA

We further selected the significantly upregulated miRNA and those mRNA genes with the top 5% most negative PTc and at least 1.5-fold exonic fraction reduction for the LIN-M vs. SOY-M contrast for miRNA-mRNA target prediction (Supplementary Table S5a). Out of the 11 mRNA highlighted by EISA (Table 1), 8 of them (72.73%, Table 1) were targeted at least once by 24 out of the 33 (72.73%) upregulated miRNA in SOY-M piglets with respect to LIN-M piglets (Supplementary Table S5b), providing a total of 34 8mer, 59 7mer-m8, and 43 7mer-A1 predicted miRNA binding sites (Supplementary Table S5c). The miRNA with the highest number of putative miRNA-mRNA interactions among the 3′ UTR of the targeted mRNA transcripts was *ssc-miR-29b*, with six predicted interactions (Supplementary Table S5b). This was followed by *ssc-miR-214-5p* with five and *ssc-miR-142-5*, *ssc-miR-221-5p, ssc-miR-29a-3p*, *ssc-miR-204*, and *ssc-miR-195* with four interactions, respectively (Supplementary Table S5b). Among this set of eight targeted mRNA, ST8 alpha-*N*-acetylneuraminide alpha-2,8-sialyltransferase 2 (*ST8SIA2*) showed the highest number of putative miRNA binding sites (13 out of 33; 39.39%), whereas both albumin (*ALB*) and serine protease 12 (*PRSS12*) showed 12 putative miRNA binding sites (36.36%) and homeobox D8 (*HOXD8*) reported a total of 9 (27.27%) (Supplementary Table S5c).

With regard to the reversed SOY-M vs. LIN-M contrast (where we took SOY-M piglets as the reference group), 60 out of the 97 (61.86%) mRNA transcripts with the top 5% most negative PTc scores and displaying at least 1.5-fold ΔEx reduction in LIN-M piglets were targeted by at least one of the reported significantly upregulated miRNA in LIN-M piglets with respect to SOY-M piglets (Supplementary Table

Table 1. Genes downregulated in SOY-M piglets with respect to LIN-M piglets and with the top 5% most negative posttranscriptional (PTc) scores and at least 1.5-fold exonic fraction (ΔEx) reduction from *longissimus dorsi* skeletal muscle samples

Gene ID	Gene	ΔEx[1]	PTc[2]	DE[3]	miRNA target
ENSSSCG00000050235		−1.484	−5.827		
ENSSSCG00000027428	*ENHO*	−0.738	−4.625	×	×
ENSSSCG00000039271	*ST8SIA2*	−1.306	−4.558	×	×
ENSSSCG00000009114	*PRSS12*	−0.797	−3.208		×
ENSSSCG00000005938	*COL22A1*	−0.636	−3.053		×
ENSSSCG00000022868	*KCTD4*	−0.934	−2.898	×	×
ENSSSCG00000041170		−0.97	−2.413		
ENSSSCG00000003527	*EPHB2*	−0.679	−2.256		×
ENSSSCG00000008948	*ALB*	−0.738	−2.089		×
ENSSSCG00000036379		−1.477	−1.790		
ENSSSCG00000040349	*HOXD8*	−0.816	−1.676		×

[1]ΔEx, exonic fraction increment ($Ex_2 - Ex_1$) in the $\log_2$ scale when comparing exon abundances in LIN-M (Ex_1) vs. SOY-M (Ex_2) piglets.
[2]PTc, posttranscriptional signal (ΔEx − ΔInt) after z-score normalization.
[3]DE, significantly differentially expressed (|FC| > 1.5; q-value < 0.05).
The "×" symbol indicates significantly downregulated genes according to their exonic counts after DE analyses, as well as those mRNA genes targeted by at least one of the significantly upregulated miRNA.

S6a). This set of 60 mRNA was targeted at least once by all 29 miRNA upregulated in LIN-M piglets (and, conversely, downregulated in SOY-M piglets, Supplementary Tables S4 and S6b). A total of 95 8mer, 303 7mer-m8, and 280 7mer-A1 predicted putative miRNA binding sites were detected between the 3′ UTR of the 60 targeted mRNA transcripts and the 29 upregulated miRNA (Supplementary Table S6c). *Ssc-miR-532-3p* was the miRNA putatively targeting the highest number of mRNA transcripts (18 out of the 60, 30%), whereas *ssc-miR-885-3p* targeted 16 out of 60 mRNA (26.67%, Supplementary Table S6b). The tripartite motif containing 14 (*TRIM14*) was the transcript concentrating the highest number of putative binding sites for different upregulated miRNA, totaling 18 out of 29 miRNAs predicted as binding to its 3′ UTR, followed by transmembrane protein 71 (*TMEM71*) and the von Willebrand factor A domain containing 5A (*VWA5A*) both with a total of 15 miRNA putatively targeting them, and interleukin-2 receptor subunit alpha (*IL2RA*) with 14 miRNA, respectively (Supplementary Table S6c).

Exonic and intronic correlations of mRNA and miRNA genes

To further investigate the observed predicted miRNA posttranscriptional regulation, we calculated Pearson's pairwise correlation coefficients (r) between the normalized $\log_2$ expression values of upregulated miRNA and the exonic and intronic fractions of their putative targeted mRNA transcripts with high posttranscriptional signals. We then took the difference from exonic and intronic correlation values ($\Delta r = r_{ex} - r_{int}$) to assess the strength of correlation change in the exonic fraction with respect to the intronic fraction. Only those miRNA-mRNA pairs with putative predicted interactions were considered.

(1) LIN-M vs. SOY-M contrast: Based on the correlation values, the energy homeostasis associated (*ENHO*) gene displayed a complete switch in correlation values ($\Delta r = -0.92$) from positive intronic correlation ($r_{int} = 0.03$) to highly negative exonic correlation ($r_{ex} = -0.89$) compared to *ssc-miR-214-5p* expression (Supplementary Table S7a). This mRNA also demonstrated a strong negative exonic correlation with two more miRNA (*ssc-miR-29a-3p* and *ssc-miR-29b*). In addition, the ephrin type-B receptor 2 (*EPHB2*), *ST8SIA2*, and *HOXD8* showed a total reversal of correlation values to a few upregulated miRNA such as *ssc-miR-23a*, *ssc-miR-221-5p*, *ssc-miR-218b*. A complete list of exonic, intronic, and change in correlation values of targeted genes and upregulated miRNA for LIN-M vs. SOY-M is shown in Supplementary Table S7a.

(2) SOY-M vs. LIN-M contrast: The top 2 pairs that showed the most negative change in correlation values were the calcineurin like EF-hand protein 2 (*CHP2*) and *ssc-miR-532-5p*, as well as CTTNBP2 n-terminal like gene (*CTTNBP2NL*) and *ssc-miR-323*, with Δr at -0.99 and -0.97, respectively. Further details are included in Supplementary Table S7b.

Functional analysis and pathway enrichment of differentially expressed genes

A total of 521 significant unique GO terms (q-value < 0.05) were detected from the differentially expressed genes related to LIN-M and SOY-M male piglets. Most of the significant GO terms were associated with immune response regulation and activation, along with carboxylic acid and polysaccharide metabolic and biosynthetic pathways. Some of these, to mention a few, are as follows: innate immune response (*GO:0045087*), regulation of cytokine-mediated signaling pathway (*GO:0001959*), regulation of alpha-beta T cell activation (*GO:0046634*), B cell differentiation (*GO:0030183*), positive regulation of interleukin-4 production (*GO:0032753*), unsaturated fatty acid biosynthetic process (*GO:0006636*), and glycogen metabolic process (*GO:0005977*). A full list of enriched GO terms is shown in Supplementary Table S8.

Association between fatty acids profile of LD muscle, PTc genes and upregulated miRNA

We performed correlation analyses among genes with the top 5% negative PTc scores and at least 1.5-fold reduction in ΔEx values, significantly upregulated miRNA and the PUFA profiles of LD skeletal muscle (Supplementary Table S1a) for both LIN-M vs. SOY-M and SOY-M vs. LIN-M contrasts. Heatmap correlation plots were created to visualize paired correlations for 1) PUFA vs. mRNA genes (Figure 2a), 2) PUFA vs. miRNA (Figure 2b), and 3) mRNA genes vs. miRNA (Figure 2c). Likewise, heatmap plots for LIN-M piglets are shown in Supplementary Figure S1a, 1b, and 1c. Our results highlighted for both SOY-M and LIN-M an overall negative correlation between the expression of posttranscriptionally downregulated mRNA and significantly upregulated miRNA, with the exception of collagen type XXII alpha 1 chain (*COL22A1*) and *ALB* mRNA in SOY-M piglets (Figure 2c), and lipase G (*LIPG*) and adiponectin (*ADIPOQ*) mRNA in LIN-M piglets (Supplementary Figure S1c).

In SOY-M piglets, a clear positive correlation and clustering pattern was observed between individual n-3 PUFA such as alpha-linolenic acid (C18:3 n-3, **ALA**) eicosatrienoic acid (C20:3 n-3, **ETA**), and eicosapentaenoic acid (C20:5 n-3, **EPA**), including the overall n-3 phenotype, and mRNA genes with negative PTc score, with the exception of *ALB* and *COL22A1* mRNA, as shown in Figure 2a. Moreover, we

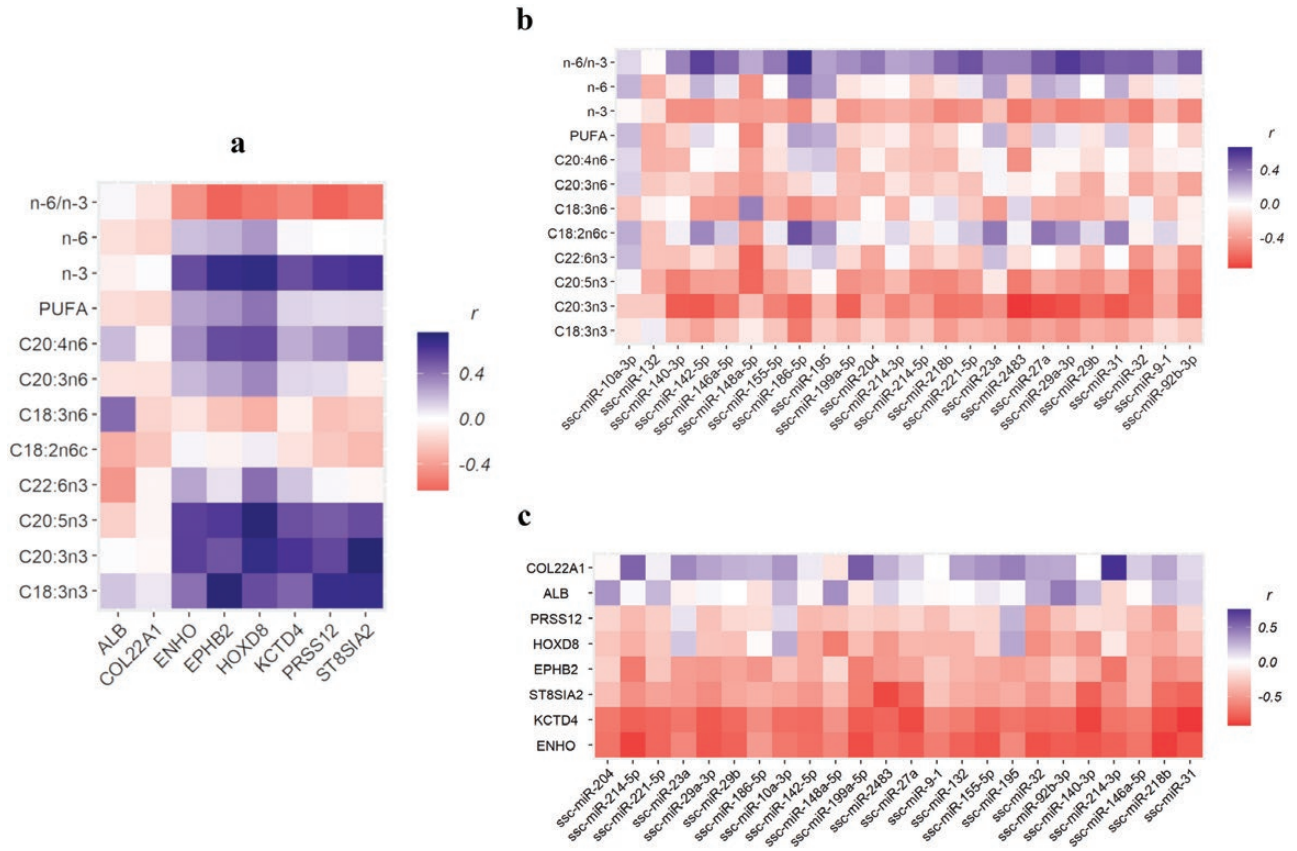

Figure 2. Heatmaps showing correlation among mRNA genes with the top 5% negative PTc scores and at least 1.5-fold reduction in ΔEx values, upregulated miRNA and PUFA profiles of *longissimus dorsi* skeletal muscle in LIN-M vs. SOY-M piglets; (a) PUFA vs. mRNA genes; (b) PUFA vs. miRNA; and (c) mRNA genes vs. miRNA.

observed a predominantly negative correlation between most posttranscriptionally downregulated genes and n-6 PUFA, mainly driven by two of them—linoleic acid (C18:2 n-6 *cis*, **LA**) and gamma-linoleic acid (C18:3 n-6, **GLA**), as well as with the ratio between n-6/n-3 PUFA (Figure 2a). Similar negative anticorrelated patterns were also detected among PUFA and significantly upregulated miRNA (Figure 2b). In this case, while the same n-3 PUFA (ALA, ETA, and EPA) were mainly involved in the observed inverse relationship, gamma-linolenic acid (C18:3 n-6, GLA), dihomo-gamma-linoleic acid (C20:3 n-6, **DGLA**) and arachidonic acid (C20:4 n-6, **AA**) but not linoleic acid (C18:2 n-6 *cis*, LA) was the PUFA driving the anticorrelation for the n-6 series (Figure 2b). Besides, contrary to what was observed for n-6/n-3 ratio and mRNA genes with high posttranscriptional downregulation signals, an overall positive correlation was observed between n-6/n-3 PUFA ratio and significantly upregulated miRNAs (Figure 2b).

The significantly upregulated miRNA in LIN-M piglets showed a clear negative correlation with posttranscriptionally downregulated mRNA, except for *LIPG* and *ADIPOQ* transcripts (Supplementary Figure S1a). Moreover, n-3 ALA, ETA and GLA fatty acids drove the observed negative correlation with mRNA genes, except for *LIPG*. DGLA and AA, but not LA and GLA, fatty acids in the n-6 series showed a clear anticorrelation with posttranscriptionally downregulated mRNA and significantly upregulated miRNA in LIN-M piglets (Supplementary Figure S1b and S1c).

Identifying posttranscriptional regulation in LD muscle from female piglets

RNA-Seq data for female piglets obtained around 100 million reads per sample. From these, ~97 million reads per sample were successfully mapped to the Sscrofa11.1 reference assembly. Besides, around 9.5 million reads per sample were kept from small RNA-Seq data after length filtering (18 to 25 nts), from which ~5.9 million reads (62%) were successfully mapped to the Sscrofa11.1 reference assembly. Approximately 79% of the mapped reads from RNA-Seq were assigned to exonic regions, while only around 3.7% of mapped reads overlapped intronic regions. With regard to small RNA-Seq data, ~75% of the mapped reads between 18 and 25 nts were successfully assigned to porcine miRNA.

Using edgeR, we obtained a total of 11,025 expressed genes based on their exonic fraction, and 33 of them were highlighted as significantly differentially expressed with an absolute FC value greater than 1.5 and a *q*-value less than 0.05. The identified differentially expressed genes were comprised of only upregulated genes in SOY-F piglets with respect to LIN-F piglets (Figure 3) and summarized in Supplementary Table S9a. A full list of exonic-based differential expression analysis in SOY-F piglets is shown in Supplementary Table S9b. Only one miRNA (ssc-miR-142-5p) was deemed to be significantly upregulated (FC > 1.5 and *q*-value < 0.05) in SOY-F piglets (Supplementary Table S10).

EISA highlighted 30 genes within the top 5% most negative PTc scores and at least 1.5-fold ΔEx reduction in

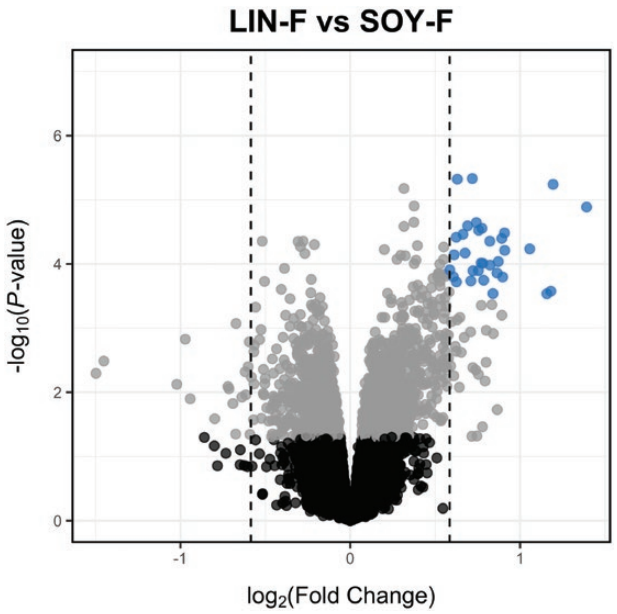

Figure 3. Volcano plot showing differentially expressed genes (fold change > |1.5| and *q*-value < 0.05) in response to extreme n-6/n-3 PUFA ratio in *longissimus dorsi* skeletal muscle from LIN-F and SOY-F female piglets. Genes with *P*-value > 0.05 are depicted in black. Upregulated genes (blue) correspond to genes overexpressed in SOY-F group.

SOY-F piglets, as shown in Supplementary Table S11. None of these were either upregulated or downregulated after canonical DE analyses. Furthermore, 6 out of the 30 (20%) mRNA transcripts were predicted as being targeted by the only upregulated miRNA found, *ssc-miR-142-5p*, totaling 7 7mer-m8 and 4 7mer-a1 putative binding sites in their 3′ UTR (Supplementary Table S12a and S12b). ST8 alpha-*N*-acetyl-neuraminide alpha-2,8-sialyltransferase 2 (*ST8SIA2*) was the mRNA with the highest number of 7mer-m8 and 7mer-A1 predicted binding sites for the upregulated miRNA *ssc-miR-142-5p*.

The posttranscriptional regulation between the targeted mRNA transcripts and the upregulated miRNA was further illustrated using the change in correlation values from intronic to exonic regions (i.e., $\Delta r = r_{ex} - r_{int}$). Most of the Δr values were negative, suggestive of an overall downregulatory effect of *ssc-miR-142-5p* over the predicted targeted mRNAs (Supplementary Table S13). Moreover, functional analysis and pathway enrichment analyses identified 15 significant unique GO terms (*q*-value < 0.05) from the exonic-based differentially expressed genes among female piglets (Supplementary Table S14). These biological pathways were mostly associated with regulation and activation of immune response such as T-cell mediated immunity (*GO:0002456*), positive regulation of interleukin-2 production (*GO:0032743*), and positive regulation of alpha-beta T cell activation (*GO:0046635*).

Correlation heatmaps for the LIN-F vs. SOY-F contrast were summarized in Supplementary Figure S2a, S2b, and S2c. Two of the analyzed n-3 PUFA (i.e., ALA and ETA) demonstrated an overall positive correlation to all of the EISA-detected downregulated mRNA genes, except for *PDZD9* (Supplementary Figure S2a), while a clear negative correlation with most of the remaining PUFA was observed. Moreover, all analyzed PUFA except for ETA and n-6/n-3 PUFA ratio displayed a positive correlation with the upregulated *ssc-miR-142-5p* (Supplementary Figure S4b). In general, all the genes with most negative PTc values according to EISA showed a negative correlation with the overexpressed miRNA in SOY-F piglets (Supplementary Figure S2c).

Discussion

Different set of genes between DE and exon–intron split analyses

Canonical differential expression analyses of exonic-based reads generally highlighted different sets of genes compared to those with strong posttranscriptional signals detected by EISA. Nevertheless, around 3 out of 11 (27.27%) of genes in LIN-M vs. SOY-M and 22 out of 97 (22.68%) of genes in SOY-M vs. LIN-M were shared between the two methodologies. Furthermore, the intronic and exonic correlation analysis between mRNA and miRNA reads in SOY-M vs. LIN-M (Supplementary Table S7b) established a more robust and clearer miRNA-driven posttranscriptional repression at the exon level compared to the more limited, yet strong regulatory signals elicited in LIN-M vs. SOY-M contrast (Supplementary Table S7a). Such discrepancy could be attributed to the overall stronger and varied upregulation of miRNA observed in LIN-M piglets.

Although no downregulated genes were detected in LIN-F vs. SOY-F after canonical DE analyses, EISA highlighted 30 genes among the top 5% negative PTc scores with an at least 1.5-fold ΔEx reduction (Supplementary Table S11). However, the posttranscriptional signals from female piglets were not as strong and clear as those from the males. The correlation values among miRNA-mRNA pairs remained negative both across intronic and exonic regions (Supplementary Table S13), indicative of mixed transcriptional and posttranscriptional downregulation signals at play that might have confounded our analyses. Moreover, we obtained only significantly upregulated mRNA and one overexpressed miRNA in the SOY-F group after canonical DE analyses. Such difference in the observed posttranscriptional regulation and differential expression of genes between male and female piglets could be associated to sex-specific metabolic responses to n-6/n-3 PUFA ratio. Multiple reports have demonstrated sex-dependent gene regulation guided by miRNA, transcription factors and other small noncoding RNAs activity, which might underline sex-specific regulatory processes in both health and disease states (Gershoni and Pietrokovski, 2017; Rounge et al., 2018). In addition, there is evidence showing the relationship between sex, sex hormones, and regulation of biological processes, including lipid-related and inflammatory-induced immunity and health disorders in humans (Klein and Flanagan, 2016; Phelps et al., 2019; Hägg and Jylhävä, 2021). Nevertheless, given the prepuberal age of the piglets analyzed, the observed differences between male and female animals might be probably due to technical or biological biases inherent to the experimental design. Regarding the PUFA considered in our experiment, the two omega PUFA series (n-3 and n-6) have antagonistic inflammatory effect and may produce metabolites that can regulate and balance one another (Schmitz and Ecker, 2008). Additional intrinsic factors such as genomics differences, as well as nutritional interventions have the possibility to change, rewire, and/or influence the overall expression profile of mRNA and miRNA (Butler, 2014). Regardless, EISA was able to provide an additional perspective on the

miRNA-driven regulation of gene expression that is complimentary to standard differential expression analyses.

Target prediction highlighted regulatory function of miRNA in response to PUFA

In SOY-M piglets, most of the genes displaying the top 5% most negative PTc scores with at least 1.5-fold exonic fraction reduction (8 out of 11, 77.73%) showed at least one binding site for the majority of significantly upregulated miRNA (24 out of 33, 72.73%). The *ssc-miR-29b* was predicted to bind the 3′ UTR of six out of the eight targeted mRNA genes and could potentially regulate their expression (Supplementary Table S5b). The *miR-29b*, a member of the *miR-29* family, targets several mRNA modulating a wide range of physiological processes including cell proliferation and apoptosis (Chung et al., 2022) or angiogenesis (Hasegawa et al., 2017). Overexpression of *miR-29b* could be related to the excess of n-6-derived metabolites in piglets fed with SOY diet, which might stimulate angiogenesis by promoting oncogenic growth factors expression (Kang and Liu, 2013). Previous reports also revealed that *miR-29b* can regulate the expression of pro-inflammatory cytokines and its relationship with inflammation and the immune response (Zhang et al., 2018).

Sixty out of 97 (61.86%) genes highlighted by EISA as posttranscriptionally downregulated in LIN-M piglets were predicted as targets of at least one among all the upregulated miRNA in LIN-M piglets, and 18 of these were linked to *ssc-miR-532-3p* (Supplementary Table S6b). Several studies have shown the anti-cancer properties of *miR-532-3p*, which can inhibit and suppress the malignancy, metastasis, and proliferation of different cancer cell types (i.e., ovary, prostate, skin, lymph nodes) (Feng et al., 2019; Wa et al., 2020; Tuo et al., 2022). These anti-carcinogenic characteristics could be attributed and might be triggered by the antioxidant and anti-inflammatory functions of n-3 PUFA (Leghi and Muhlhausler, 2016). Our results also highlighted 6 genes that could be targeted by the upregulated miRNA *ssc-miR-142-5p* in SOY-F piglets. This miRNA has been related to human chronic inflammatory and autoimmune diseases and can be induced by immune response regulators such as interleukin-4 and interleukin-13 (Su et al., 2015; Bayomy et al., 2022). Although *ssc-miR-142-5p* was found to be upregulated in SOY-F, its expression was generally low (Supplementary Table S10). While the detected posttranscriptional signals might be weak, this miRNA was still predicted to target a few mRNA transcripts that belonged to the strongest observed downregulation based on ΔEx values and PTc scores in SOY-F piglets (Supplementary Table S11), while such effect was not captured by canonical differential expression analyses. This demonstrates the importance of performing analyses to gene expression data other than DE analyses, to provide a more comprehensive landscape of the regulatory effects at play.

It is worth noting that, for some of the predicted miRNA-mRNA interactions, there was a clear negative correlation between the given miRNA and the targeted mRNA at the exonic level, as expected for any posttranscriptional regulatory effect happening in the cytoplasm after intron splicing. In this way, when analyzing the correlation between the putative regulatory miRNA and the targeted mRNA at the intronic level, the observed anticorrelation was lost or even of opposite sign compared to that of the exonic fraction. This is the case, for instance, of *ENHO*, *HOXD8*, *EPHB2*, and *ST8SIA2* in SOY-M piglets (Supplementary Table S7a), or *CHP2* and *CTTNBP2NL* in LIN-M piglets (Supplementary Table S7b). The observed predominance of gene expression anticorrelation between these mRNA and some of their predicted targeting miRNA at the exonic but not at the intronic level might be indeed a good indicator of the reliability of the predicted interaction, as no intronic expression response should be expected, in principle, driven by miRNA acting at the posttranscriptional level.

Association between genes with the strongest posttranscriptional downregulation and biological processes related to lipid metabolism and immunomodulation

EISA highlighted multiple genes with relevant posttranscriptional downregulation in LIN-M vs. SOY-M. The *ST8SIA2* gene displayed one of the most negative PTc scores. Additionally, it was detected as significantly downregulated by canonical DE analyses, and harbored the highest number of putative binding sites in its 3′ UTR for thirteen out of the 33 upregulated miRNA in SOY-M piglets. The *ST8SIA2* gene encodes a type II membrane protein that catalyzes the transfer of sialic acid to N-linked oligosaccharides and glycoproteins (Yang et al., 2022). This function is relevant since studies have shown that a deficiency in sialic acid or N-glycans is associated with oxidative (Cho et al., 2017) and inflammatory stress (Woodward et al., 2019), which could be expected in soy-based diets where the n-6/n-3 PUFA ratio is increased. Reports on mice have shown that deficiency of *ST8SIA2*, combined with the decreased expression of insulin growth-like factor 1 receptor, is correlated to lethality (Ikegami et al., 2019). *ST8SIA2*was also found to be targeted by the single one overexpressed miRNA in SOY-F piglets (*ssc-miR-142-5p*, Supplementary Table S10).

Other relevant genes that were both posttranscriptionally repressed and significantly downregulated after EISA and canonical DE analyses were the energy homeostasis associated (*ENHO*) and potassium channel tetramerization domain containing 4 (*KCTD4*) genes. *ENHO* encodes a peptide hormone called adropin, which plays a role in regulating lipid and glucose homeostasis and prevents hyperinsulinemia, dyslipidemia, and impaired glucose tolerance (Kumar et al., 2008; Es-haghi et al., 2021). Adropin deficiency has been linked with increased adiposity, insulin resistance, and metabolic defects (Ganesh-Kumar et al., 2012; Chen et al., 2017). Besides, *KCTD4* belongs to a gene family that is associated to cancer, neurological diseases, obesity, and metabolic disorders (Ng et al., 2010; Liu et al., 2013; Teng et al., 2019).

We also detected several other miRNA-targeted transcripts with negative PTc scores correlated to specific lipid-related biological processes, such as ephrin type-B receptor 2 (*EPBH2*) which regulates key proteins involved in maintaining lipid and glycogen homeostasis (Jiang et al., 2015; Morales et al., 2021), or *HOXD8*, involved in carcinogenesis, tumor suppression (Zhang et al., 2021) and adipogenesis regulation (Kumar et al., 2021). Nevertheless, the EISA approach also highlighted other lipid-related genes, such as *COL22A1* and *ALB*, as showing high posttranscriptional signals However, we did not observe the expected anticorrelation with upregulated miRNA putatively targeting them, as shown in Figure 2c. Even though these transcripts (*COL22A1* and *ALB*) harbored predicted miRNA binding sites, their expression showed confounding patterns that might have elicited a false positive detection by EISA and/or we obtained a false

interaction by miRNA binding site prediction to their 3′ UTRs (Pinzón et al., 2017).

With regard to the opposite SOY-M vs. LIN-M contrast, the mRNA with the most negative PTc score and that gathered putative binding sites to fifteen significantly upregulated miRNA was *TMEM71* (Supplementary Table S6a). This gene encodes a transmembrane protein that is involved in immune and inflammatory response (Wang et al., 2019). *CHP2*, which is associated with cancer progression and cellular functions regulation (Li et al., 2008; Di Sole et al., 2012) and could be inhibited by PUFA (Tokheim and Martin, 2006), further displayed a clear posttranscriptional downregulation, demonstrating a strong negative correlation with *ssc-miR-532-5p* at the exonic level (Supplementary Table S7b). Furthermore, our results highlighted multiple cluster of differentiation (*CD*) genes, including *CD3*, *CD7*, *CD22*, *CD48*, *CD68*, *CD86*, and *CD163*, which are commonly associated with cytokine generation, T-cell regulation, cancer immunotherapy, immunological response, and/or inflammation (McArdel et al., 2016; Zeibig et al., 2019). EISA provided a few more genes that were associated with immune system function such as interleukin-2 receptor α (*IL2RA*) (Buhelt et al., 2021); interferon regulatory factor 4 (*IRF4*) (Sundararaj et al., 2022); kinesin family member 21B (*KIF21B*) (Hooikaas et al., 2020), G protein-coupled receptor 176 (*GPR176*) (Goto et al., 2017); and heme oxygenase 1 (*HMOX1*) (Gao et al., 2022).

EISA highlighted additional mRNA genes that were associated with, but not limited to, lipid metabolism, lipoprotein metabolism, atherosclerosis, and obesity, such as porcine-specific cytochrome P450 family 3 subfamily A member 22 (*CYP3A22*) (Konkel and Schunck, 2011), cadherin related family member 1 (*CDHR1*) and phosphatidylinositol-4,5-bisphosphate 3-kinase catalytic subunit delta (*PIK3CD*) (Ballas, 2018; Virk et al., 2022). We also obtained a few genes with negative PTc scores that were not clearly downregulated by upregulated miRNA—*LIPG* and *ADIPOQ* genes. Likewise, EISA provided some mRNA genes that were posttranscriptionally repressed and significantly downregulated after DE analysis, but were not targeted by any significantly upregulated miRNA. Although miRNA are important posttranscriptional regulators, other posttranscriptional effectors such as long noncoding RNAs, circular RNAs, or RNA binding proteins may also be at play (Van Assche et al., 2015; Bose and Ain, 2018). Moreover, additional miRNAs with active biological functionality might not have been captured as significantly upregulated and hence missed in our analyses.

PUFA abundance in skeletal muscle is associated with the expression of downregulated mRNA and upregulated miRNA

Correlation analyses allowed us to link the expression profile of genes showing high posttranscriptional signals, upregulated miRNA, and the analyzed PUFA profiles of porcine skeletal muscle. In general, the highlighted mRNA and miRNA showed a negative relationship in both SOY-M and LIN-M piglets (Figure 2c and Supplementary Figure S1c), as the overexpression of these miRNA could potentially suppress or downregulate the targeted mRNA transcripts (Bartel, 2018). We observed a clear cluster of positive correlation (SOY-M piglets) among mRNA showing strong posttranscriptional downregulation and n-3 PUFA such as ALA, ETA, and EPA. Conversely, n-6 PUFA showed the opposite pattern, mostly driven by LA and GLA fatty acids. The observed association between PUFA concentration and expression of mRNA and miRNA agrees well with previous reports on the influence of PUFA in altering gene regulatory networks (Zheng et al., 2015; Xie et al., 2021).

Using the same male and female piglets as in the current study, our previous report (Manaig et al., 2022) showed how the relative proportions of n-3 PUFA (i.e., ALA, ETA, EPA, and DHA) were significantly higher in LD skeletal muscle in LIN compared to SOY diets in piglets, and no significant differences were observed among the n-6 PUFA. This might explain the weaker correlation driven by n-6 PUFA on mRNA and miRNA obtained in the present study. Moreover, as previously reported (Manaig et al., 2022), the dietary oils that were incorporated in sow's gestation and lactation diets were soybean oil and linseed oil. Fatty acid composition analyses also showed that soybean oil contains high proportion of the LA n-6 PUFA, while linseed oil is composed of mostly the n-3 PUFA ALA (Manaig et al., 2022). Our results highlighted ALA (n-3) and LA (n-6) as two of the main drivers of the overall phenotypic variance observed in porcine skeletal muscle in response to changes in PUFA composition in piglet's diet. As the most abundant n-3 and n-6 PUFA in linseed (ALA) and soybean (LA) oils, they can modulate gene expression related to their antagonistic inflammatory functions and lipid-related metabolic processes (Schmitz and Ecker, 2008; Smink et al., 2012). Studies on mice demonstrated how varying concentrations of ALA and LA might differentially influence the expression profiles of genes and proteins in muscle tissue (Rajna et al., 2018). Besides, other additional relevant PUFA we found were ETA (n-3), which is able trigger the downregulation of genes related to inflammation (Jin et al., 2010; Chen et al., 2015), EPA (n-3), which modulates peroxisome proliferator-activated receptors and genes related to dyslipidemia and inflammation (Gillies et al., 2012), or GLA (n-6), that is able to decrease the expression of pro-inflammatory cytokines and related mediators (Youn et al., 2018).

Conclusion

The use of EISA highlighted posttranscriptional changes in mRNA genes expressed in porcine skeletal muscle. Although there was a limited overlap between EISA and canonical DE analyses outputs, EISA provided additional and biologically meaningful information about changes in mRNA expression that were not captured by DE results, coupled with miRNA-driven repression evidence by target binding prediction. Individual n-3 and n-6 PUFA may play a vital role in gene and miRNA expression and regulation. Both EISA and differential expression analyses highlighted genes and miRNA that were associated to lipid-mediated and inflammatory-induced biological processes, which could be attributed to the pro- and anti-inflammatory functions of n-6 and n-3 PUFA, respectively.

Supplementary Data

Supplementary data are available at *Journal of Animal Science* online.

Acknowledgments

This work was supported by the European Union Horizon 2020 Research and Innovation programme H2020-MSCA-ITN-2017-EJD: Marie Skłodowska-Curie Innovative

Training Networks (European Joint Doctorate) – Grant agreement: 765423—MANNA. Additionally, it was supported by the Spanish Ministerio de Ciencia e Innovación (MICINN) and the Fondo Europeo de Desarrollo Regional (FEDER) with project references: AGL2017-82641-R and PID2020-112677RB-C22. We also acknowledge the support of the Spanish Ministerio de Economía y Competitividad for the "Severo Ochoa" Programme for Centres of Excellence in R&D (Project CEX2019-000902-S) to the Centre for Research in Agricultural Genomics (CRAG) and to the programmes of Centres de Recerca de Catalunya (CERCA). Funding organizations were not involved in the execution of the project or the interpretation of results. All experimental protocols were approved by the ethical committee of the University of Milan (OPBA 22/2020). We also thank for help of Dr. Eleonora Munari and the University of Milan farm personnel with the in vivo trials, and Dr. Sara Panseri and Giacomo Mosconi for fatty acid analysis.

Conflict of Interest Statement

No conflict of interest, financial, or otherwise is declared by the authors.

Data Availability

The data underlying this article are subject to an embargo of 12 months or when the manuscript is published. Once the embargo expires, the data will be available at NCBI Sequence Read Archive (SRA) repository under BioProject ID PRJNA954344. https://dataview.ncbi.nlm.nih.gov/object/PRJNA954344?reviewer=dgf0k82f7uqcmqnqe5iasv493e

Literature Cited

Andrews, S. 2010. FastQC: a quality control tool for high throughput sequence data [Computer software]. Babraham Bioinformatics. http://www.bioinformatics.babraham.ac.uk./projects/fastqc/.

Ballas, Z. K. 2018. The editors' choice. *J. Allergy Clin. Immunol.* 141:2015–2016. doi:10.1016/j.jaci.2018.04.019.

Bartel, D. P. 2018. Metazoan MicroRNAs. *Cell.* 173:20–51. doi:10.1016/j.cell.2018.03.006.

Bayomy, N. R., W. M. Abo Alfottoh, S. A. Ali Eldeep, A. M. S. Ibrahim Mabrouk Mersal, H. M. A. Abd El-Bary, and E. M. Abd El Gayed. 2022. Mir-142-5p as an indicator of autoimmune processes in childhood idiopathic nephrotic syndrome and as a part of MicroRNAs expression panels for its diagnosis and prediction of response to steroid treatment. *Mol. Immunol.* 141:21–32. doi:10.1016/j.molimm.2021.11.004.

Benjamini, Y., and Y. Hochberg. 1995. Controlling the false discovery rate: a practical and powerful approach to multiple testing. *J. R. Stat. Soc. Ser. B.* 57:289–300. doi:10.1111/j.2517-6161.1995.tb02031.x.

Bindea, G., B. Mlecnik, H. Hackl, P. Charoentong, M. Tosolini, A. Kirilovsky, W. H. Fridman, F. Pagès, Z. Trajanoski, and J. Galon. 2009. ClueGO: a Cytoscape plug-in to decipher functionally grouped gene ontology and pathway annotation networks (Version 2.5.4) [Computer software]. *Bioinformatics.* 25:1091–1093. doi:10.1093/bioinformatics/btp101.

Bose, R., and R. Ain. 2018. Regulation of transcription by circular RNAs. *Adv. Exp. Med. Biol.* 1087:81–94. doi:10.1007/978-981-13-1426-1_7.

Buhelt, S., H. M. Laigaard, M. R. von Essen, H. Ullum, A. Oturai, F. Sellebjerg, and H. B. Søndergaard. 2021. IL2RA methylation and gene expression in relation to the multiple sclerosis-associated gene variant rs2104286 and soluble IL-2Rα in CD8+ T cells. *Front. Immunol.* 12:676141. doi:10.3389/fimmu.2021.676141.

Butler, G. 2014. Manipulating dietary PUFA in animal feed: implications for human health. *Proc. Nutr. Soc.* 73:87–95. doi:10.1017/S0029665113003790.

Chen, S. J., L. T. Chuang, and S. N. Chen. 2015. Incorporation of eicosatrienoic acid exerts mild anti-inflammatory properties in murine RAW264.7 cells. *Inflammation.* 38:534–545. doi:10.1007/s10753-014-9960-8.

Chen, S., K. Zeng, Q. C., Liu, Z. Guo, S. Zhang, X. R. Chen, J. H. Lin, J. P. Wen, C. F. Zhao, et al. 2017. Adropin deficiency worsens HFD-induced metabolic defects. *Cell Death Dis.* 8:e3008. doi:10.1038/cddis.2017.362.

Cho, A., M. Christine, V. Malicdan, M. Miyakawa, I. Nonaka, I. Nishino, and S. Noguchi. 2017. Sialic acid deficiency is associated with oxidative stress leading to muscle atrophy and weakness in GNE myopathy. *Hum. Mol. Genet.* 26:3081–3093. doi:10.1093/hmg/ddx192.

Chung, H. K., J. N. Rao, and J. Y. Wang. 2022. Regulation of gut barrier function by RNA-binding proteins and noncoding RNAs. In: Kenakin, T., editor. *Comprehensive pharmacology*. Amsterdam, Netherlands: Elsevier; p. 194–213.

Costa-Silva, J., D. Domingues, and F. M. Lopes. 2017. RNA-Seq differential expression analysis: an extended review and a software tool. *PLoS One.* 12:e0190152. doi:10.1371/journal.pone.0190152.

Di Sole, F., K. Vadnagara, O. W. Moe, and V. Babich. 2012. Calcineurin homologous protein: a multifunctional Ca 2+ -binding protein family. *Am. J. Physiol. Renal. Physiol.* 303:F165–F179. doi:10.1152/ajprenal.00628.2011.

Es-haghi, A., T. Al-Abyadh, and H. Mehrad-Majd. 2021. The clinical value of serum adropin level in early detection of diabetic nephropathy. *Kidney Blood Press. Res.* 46:734–740. doi:10.1159/000519173.

Feng, C., H. I., So, S. Yin, X. Su, Q. Xu, and Z. Xu. 2019. MicroRNA-532-3p suppresses malignant behaviors of tongue squamous cell carcinoma via regulating CCR7. *Front. Pharmacol.* 10:940. doi:10.3389/fphar.2019.00940.

Filipowicz, W., S. N. Bhattacharyya, and N. Sonenberg. 2008. Mechanisms of post-transcriptional regulation by microRNAs: are the answers in sight? *Nat. Rev. Genet.* 9:102–114. doi:10.1038/nrg2290.

Frazee, A. C., S. Sabunciyan, K. D. Hansen, R. A. Irizarry, and J. T. Leek. 2014. Differential expression analysis of RNA-seq data at single-base resolution. *Biostatistics.* 15:413–426. doi:10.1093/biostatistics/kxt053.

Gaidatzis, D., L. Burger, M. Florescu, and M. B. Stadler. 2015. Analysis of intronic and exonic reads in RNA-seq data characterizes transcriptional and post-transcriptional regulation. *Nat. Biotechnol.* 33:722–729. doi:10.1038/nbt.3269.

Ganesh-Kumar, K., J. Zhang, S. Gao, J. Rossi, O. P. McGuinness, H. H. Halem, M. D. Culler, R. L. Mynatt, and A. A. Butler. 2012. Adropin deficiency is associated with increased adiposity and insulin resistance. *Obesity.* 20:1394–1402. doi:10.1038/oby.2012.31.

Gao, M., Z. Qi, M. Deng, H. Huang, Z. Xu, G. Guo, J. Jing, X. Huang, M. Xu, J. A. Kloeber, et al. 2022. The deubiquitinase USP7 regulates oxidative stress through stabilization of HO-1. *Oncogene.* 41:4018–4027. doi:10.1038/s41388-022-02403-w.

Georgiadi, A., and S. Kersten. 2012. Mechanisms of gene regulation by fatty acids. *Adv. Nutr.* 3:127–134. doi:10.3945/an.111.001602.

Gershoni, M., and S. Pietrokovski. 2017. The landscape of sex-differential transcriptome and its consequent selection in human adults. *BMC Biol.* 15:7. doi:10.1186/s12915-017-0352-z.

Gillies, P. J., S. K. Bhatia, L. A. Belcher, D. B. Hannon, J. T. Thompson, and J. P. Vanden Heuvel. 2012. Regulation of inflammatory and lipid metabolism genes by eicosapentaenoic acid-rich oil. *J. Lipid Res.* 53:1679–1689. doi:10.1194/jlr.M022657.

Goto, K., M. Doi, T. Wang, S. Kunisue, I. Murai, and H. Okamura. 2017. G-protein-coupled receptor signaling through Gpr176, Gz,

and RGS16 tunes time in the center of the circadian clock. *Endocr. J*. 64:571–579. doi:10.1507/endocrj.EJ17-0130.

Hägg, S., and J. Jylhävä. 2021. Sex differences in biological aging with a focus on human studies. *ELife*. 10:e63425. doi:10.7554/eLife.63425.

Hasegawa, T., H. Lewis, and A. Esquela-Kerscher. 2017. The role of noncoding RNAs in prostate cancer. In Laurence, J., editor. *Translating microRNAs to the clinic*. Cambridge, MA: Academic Press; p. 329–369.

Hooikaas, P. J., H. G. Damstra, O. J. Gros, W. E. van Riel, M. Martin, Y. T. Smits, J. V. Loosdregt, L. C. Kapitein, F. Berger, et al. 2020. Kinesin-4 KIF21B limits microtubule growth to allow rapid centrosome polarization in T cells. *eLife*. 9:e62876. doi:10.7554/eLife.62876.

Horodyska, J., K. Wimmers, H. Reyer, N. Trakooljul, A. M. Mullen, P. G. Lawlor, and R. M. Hamill. 2018. RNA-seq of muscle from pigs divergent in feed efficiency and product quality identifies differences in immune response, growth, and macronutrient and connective tissue metabolism. *BMC Genomics*. 19:791. doi:10.1186/s12864-018-5175-y.

Ikegami, K., K. Saigoh, A. Fujioka, M. Nagano, K. Kitajima, C. Sato, S. Masubuchi, S. Kusunoki, and Y. Shigeyoshi. 2019. Effect of expression alteration in flanking genes on phenotypes of *St8sia2*-deficient mice. *Sci. Rep*. 9:13634. doi:10.1038/s41598-019-50006-5.

Jiang, J., Z. H. Wang, M. Qu, D. Gao, X. -P. Liu, L. Q. Zhu, and J. Z. Wang. 2015. Stimulation of EphB2 attenuates tau phosphorylation through PI3K/Akt-mediated inactivation of glycogen synthase kinase-3β. *Sci. Rep*. 5:11765. doi:10.1038/srep11765.

Jin, X. J., E. J. Kim, I. K. Oh, Y. K. Kim, C. H. Park, and J. H. Chung. 2010. Prevention of UV-induced skin damages by 11,14,17-eicosatrienoic acid in hairless mice in vivo. *J. Korean Med. Sci*. 25:930–937. doi:10.3346/jkms.2010.25.6.930.

Kang, J. X., and A. Liu. 2013. The role of the tissue omega-6/omega-3 fatty acid ratio in regulating tumor angiogenesis. *Cancer Metastasis Rev*. 32:201–210. doi:10.1007/s10555-012-9401-9.

Kim, D., J. M. Paggi, C. Park, C. Bennett, and S. L. Salzberg. 2019. Graph-based genome alignment and genotyping with HISAT2 and HISAT-genotype. *Nat. Biotechnol*. 37:907–915. doi:10.1038/s41587-019-0201-4.

Klein, S. L., and K. L. Flanagan. 2016. Sex differences in immune responses. *Nat. Rev. Immunol*. 16:626–638. doi:10.1038/nri.2016.90.

Konkel, A., and W. H. Schunck. 2011. Role of cytochrome P450 enzymes in the bioactivation of polyunsaturated fatty acids. *Biochim. Biophys. Acta*. 1814:210–222. doi:10.1016/j.bbapap.2010.09.009.

Kozomara, A., M. Birgaoanu, and S. Griffiths-Jones. 2019. MiRBase: from microRNA sequences to function. *Nucleic Acids Res*. 47:D155–D162. doi:10.1093/nar/gky1141.

Kumar, V., M. Sekar, P. Sarkar, K. K. Acharya, and K. Thirumurugan. 2021. Dynamics of HOX gene expression and regulation in adipocyte development. *Gene*. 768:145308. doi:10.1016/j.gene.2020.145308.

Kumar, K. G., J. L. Trevaskis, D. D. Lam, G. M. Sutton, R. A. Koza, V. N. Chouljenko, K. G. Kousoulas, P. M. Rogers, R. A. Kesterson, et al. 2008. Identification of adropin as a secreted factor linking dietary macronutrient intake with energy homeostasis and lipid metabolism. *Cell Metab*. 8:468–481. doi:10.1016/j.cmet.2008.10.011.

Langmead, B., C. Trapnell, M. Pop, and S. L. Salzberg. 2009. Bowtie: ultrafast and memory-efficient alignment of short DNA sequences to the human genome. *Genome Biol*. 10:R25. doi:10.1186/gb-2009-10-3-r25.

Leghi, G. E., and B. S. Muhlhausler. 2016. The effect of n-3 LCPUFA supplementation on oxidative stress and inflammation in the placenta and maternal plasma during pregnancy. *Prostaglandins Leukot. Essent. Fat. Acids*. 113:33–39. doi:10.1016/j.plefa.2016.08.010.

Li, G. D., X. Zhang, R. Li, Y. D. Wang, Y. L., Wang, K. J. Han, X. P. Qian, C. G. Yang, P. Liu, et al. 2008. CHP2 activates the calcineurin/nuclear factor of activated T cells signaling pathway and enhances the oncogenic potential of HEK293 cells. *J. Biol. Chem*. 283:32660–32668. doi:10.1074/jbc.M806684200.

Liao, Y., G. K. Smyth, and W. Shi. 2014. featureCounts: an efficient general purpose program for assigning sequence reads to genomic features. *Bioinformatics*. 30:923–930. doi:10.1093/bioinformatics/btt656.

Liu, Z., Y. Xiang, and G. Sun. 2013. The KCTD family of proteins: structure, function, disease relevance. *Cell Biosci*. 3:45. doi:10.1186/2045-3701-3-45.

Manaig, Y. J. Y., L. Criado-Mesas, A. Esteve-Codina, E. Mármol-Sánchez, A. Castelló, A. Sanchez, and J. M. Folch. 2023. Identifying miRNA-mRNA regulatory networks on extreme n-6/n-3 polyunsaturated fatty acid ratio expression profiles in porcine skeletal muscle. *PLoS One*. 18:e0283231. doi:10.1371/journal.pone.0283231.

Manaig, Y. J. Y., S. Sandrini, S. Panseri, G. Tedeschi, J. M. Folch, A. Sánchez, G. Savoini, and A. Agazzi. 2022. Low n-6/n-3 gestation and lactation diets influence early performance, muscle and adipose polyunsaturated fatty acid content and deposition, and relative abundance of proteins in suckling piglets. *Molecules*. 27:2925. doi:10.3390/molecules27092925.

Marco, A. 2018. SeedVicious: analysis of microRNA target and near-target sites. *PLoS One*. 13:e0195532. doi:10.1371/journal.pone.0195532.

Mármol-Sánchez, E., S. Cirera, L. M. Zingaretti, M. J. Jacobsen, Y. Ramayo-Caldas, C. B. Jørgensen, M. Fredholm, T. F. Cardoso, R. Quintanilla, and M. Amills. 2022. Modeling microRNA-driven post-transcriptional regulation using exon–intron split analysis in pigs. *Anim. Genet*. 53:613–626. doi:10.1111/age.13238.

Mármol-Sánchez, E., Y. Ramayo-Caldas, R. Quintanilla, T. F. Cardoso, R. González-Prendes, J. Tibau, and M. Amills. 2020. Co-expression network analysis predicts a key role of microRNAs in the adaptation of the porcine skeletal muscle to nutrient supply. *J. Anim. Sci. Biotechnol*. 11:10. doi:10.1186/s40104-019-0412-z.

Martin, M. 2011. Cutadapt removes adapter sequences from high-throughput sequencing reads. *EMBnet J*. 17:10. doi:10.14806/ej.17.1.200.

McArdel, S. L., C. Terhorst, and A. H. Sharpe. 2016. Roles of CD48 in regulating immunity and tolerance. *Clin. Immunol*. 164:10–20. doi:10.1016/j.clim.2016.01.008.

McDermaid, A., B. Monier, J. Zhao, B. Liu, and Q. Ma. 2019. Interpretation of differential gene expression results of RNA-seq data: review and integration. *Brief. Bioinform*. 20:2044–2054. doi:10.1093/bib/bby067.

Morales, A., M. Greenberg, F. Nardi, V. Gil, S. W. Hayward, S. E. Crawford, and O. E. Franco. 2021. Loss of ephrin B2 receptor (EPHB2) sets lipid rheostat by regulating proteins DGAT1 and ATGL inducing lipid droplet storage in prostate cancer cells. *Lab. Investig*. 101:921–934. doi:10.1038/s41374-021-00583-9.

Naeli, P., T. Winter, A. P. Hackett, L. Alboushi, and S. M. Jafarnejad. 2022. The intricate balance between microRNA-induced mRNA decay and translational repression. *FEBS J*. 290:2508–2524. doi:10.1111/febs.16422.

Ng, M. C. Y., C. H. Tam, W. Y. So, J. S. Ho, A. W. Chan, H. M. Lee, Y. Wang, V. K. Lam, J. C. Chan, and R. C. W. Ma. 2010. Implication of genetic variants near NEGR1, SEC16B, TMEM18, ETV5/DGKG, GNPDA2, LIN7C/BDNF, MTCH2, BCDIN3D/FAIM2, SH2B1, FTO, MC4R, and KCTD15 with obesity and type 2 diabetes in 7705 Chinese. *J. Clin. Endocrinol. Metab*. 95:2418–2425. doi:10.1210/jc.2009-2077.

Nguyen, T. X., A. Agazzi, M. Comi, V. Bontempo, I. Guido, S. Panseri, H. Sauerwein, P. D. Eckersall, R. Burchmore, and G. Savoini. 2020. Effects of low ω6:ω3 ratio in sow Diet and seaweed supplement in piglet diet on performance, colostrum and milk fatty acid profiles, and oxidative status. *Animals*. 10:2049. doi:10.3390/ani10112049.

Ntambi, J. M., and H. Bené. 2001. Polyunsaturated fatty acid regulation of gene expression. *J. Mol. Neurosci*. 16:273–278; discussion 279. doi:10.1385/JMN:16:2-3:273.

Phelps, T., E. Snyder, E. Rodriguez, H. Child, and P. Harvey. 2019. The influence of biological sex and sex hormones on bile acid synthesis and cholesterol homeostasis. *Biol. Sex Differ*. 10:52. doi:10.1186/s13293-019-0265-3.

Pillman, K. A., K. G. Scheer, E. Hackett-Jones, K. Saunders, A. G. Bert, J. Toubia, H. J. Whitfield, S. Sapkota, L. Sourdin, H. Pham, et al. 2019. Extensive transcriptional responses are co-ordinated by microRNAs as revealed by exon–intron split analysis (EISA). *Nucleic Acids Res*. 47:8606–8619. doi:10.1093/nar/gkz664.

Pinzón, N., B. Li, L. Martinez, A. Sergeeva, J. Presumey, F. Apparailly, and H. Seitz. 2017. microRNA target prediction programs predict many false positives. *Genome Res*. 27:234–245. doi:10.1101/gr.205146.116.

Rajna, A., H. Gibling, O. Sarr, S. Matravadia, G. P. Holloway, and D. M. Mutch. 2018. Alpha-linolenic acid and linoleic acid differentially regulate the skeletal muscle secretome of obese Zucker rats. *Physiol. Genomics*. 50:580–589. doi:10.1152/physiolgenomics.00038.2018.

Ramayo-Caldas, Y., N. Mach, A. Esteve-Codina, J. Corominas, A. Castelló, M. Ballester, J. Estellé, N. Ibáñez-Escriche, A. I. Fernández, M. Pérez-Enciso, et al. 2012. Liver transcriptome profile in pigs with extreme phenotypes of intramuscular fatty acid composition. *BMC Genomics*. 13:547. doi:10.1186/1471-2164-13-547.

Robinson, M. D., D. J. McCarthy, and G. K. Smyth. 2010. edgeR: a Bioconductor package for differential expression analysis of digital gene expression data. *Bioinformatics*. 26:139–140. doi:10.1093/bioinformatics/btp616.

Robinson, M. D., and A. Oshlack. 2010. A scaling normalization method for differential expression analysis of RNA-seq data. *Genome Biol*. 11:R25. doi:10.1186/gb-2010-11-3-r25.

Rounge, T. B., S. U. Umu, A. Keller, E. Meese, G. Ursin, S. Tretli, R. Lyle, and H. Langseth. 2018. Circulating small non-coding RNAs associated with age, sex, smoking, body mass and physical activity. *Sci. Rep*. 8:17650. doi:10.1038/s41598-018-35974-4.

Sakayori, N., M. Katakura, K. Hamazaki, O. Higuchi, K. Fujii, R. Fukabori, Y. Iguchi, S. Setogawa, K. Takao, T. Miyazawa, et al. 2020. Maternal dietary imbalance between omega-6 and omega-3 fatty acids triggers the offspring's overeating in mice. *Commun. Biol*. 3:473. doi:10.1038/s42003-020-01209-4.

Schmitz, G., and J. Ecker. 2008. The opposing effects of n-3 and n-6 fatty acids. *Prog. Lipid Res*. 47:147–155. doi:10.1016/j.plipres.2007.12.004.

Shannon, P., A. Markiel, O. Ozier, N. S. Baliga, J. T. Wang, D. Ramage, N. Amin, B. Schwikowski, and T. Ideker. 2003. Cytoscape: a software environment for integrated models of biomolecular interaction networks. *Genome Res*. 13:2498–2504. doi:10.1101/gr.1239303.

Smink, W., W. J. J. Gerrits, M. Gloaguen, A. Ruiter, and J. Van Baal. 2012. Linoleic and α-linolenic acid as precursor and inhibitor for the synthesis of long-chain polyunsaturated fatty acids in liver and brain of growing pigs. *Animal*. 6:262–270. doi:10.1017/S1751731111001479.

Su, S., Q. Zhao, C. He, D. Huang, J. Liu, F. Chen, J. Chen, J. Y. Liao, X. Cui, Y. Zeng, et al. 2015. miR-142-5p and miR-130a-3p are regulated by IL-4 and IL-13 and control profibrogenic macrophage program. *Nat. Commun*. 6:8523. doi:10.1038/ncomms9523.

Sundararaj, S., S. Seneviratne, S. J. Williams, A. Enders, and M. G. Casarotto. 2022. The molecular basis for the development of adult T-cell leukemia/lymphoma in patients with an IRF4K59R mutation. *Protein Sci*. 31:787–796. doi:10.1002/pro.4260.

Teng, X., A. Aouacheria, L. Lionnard, K. A. Metz, L. Soane, A. Kamiya, and J. M. Hardwick. 2019. KCTD: a new gene family involved in neurodevelopmental and neuropsychiatric disorders. *CNS Neurosci. Ther*. 25:887–902. doi:10.1111/cns.13156.

Tokheim, A. M., and B. L. Martin. 2006. Inhibition of calcineurin by polyunsaturated lipids. *Bioorg. Chem*. 34:66–76. doi:10.1016/j.bioorg.2005.12.002.

Tuo, X., Y. Zhou, X. Yang, S. Ma, D. Liu, X. Zhang, H. Hou, R. Wang, X. Li, and L. Zhao. 2022. miR-532–3p suppresses proliferation and invasion of ovarian cancer cells via GPNMB/HIF-1α/HK2 axis. *Pathol. Res. Pract*. 237:154032. doi:10.1016/j.prp.2022.154032.

Van Assche, E., S. Van Puyvelde, J. Vanderleyden, and H. P. Steenackers. 2015. RNA-binding proteins involved in post-transcriptional regulation in bacteria. *Front. Microbiol*. 6:141. doi:10.3389/fmicb.2015.00141.

Virk, R., N. Buddenbaum, A. Al-Shaer, M. Armstrong, J. Manke, N. Reisdorph, S. Sergin, J. I., Fenton, E. D. Wallace, B. M. Ehrmann, et al. 2022. Obesity reprograms the pulmonary polyunsaturated fatty acid-derived lipidome, transcriptome, and gene-oxylipin networks. *J. Lipid Res*. 63:100267. doi:10.1016/j.jlr.2022.100267.

Wa, Q., C. Zou, Z. Lin, S. Huang, X. Peng, C. Yang, D. Ren, D. Xu, Y. Guo, Z. Liao, et al. 2020. Ectopic expression of miR-532-3p suppresses bone metastasis of prostate cancer cells via inactivating NF-κB signaling. *Mol. Ther. Oncolytics*. 17:267–277. doi:10.1016/j.omto.2020.03.024.

Wang, K., R. Y. Huang, X. Z. Tong, K. N. Zhang, Y. W. Liu, F. Zeng, H. M. Hu, and T. Jiang. 2019. Molecular and clinical characterization of TMEM71 expression at the transcriptional level in glioma. *CNS Neurosci. Ther*. 25:965–975. doi:10.1111/cns.13137.

Warr, A., N. Affara, B. Aken, H. Beiki, D. M. Bickhart, K. Billis, W. Chow, L. Eory, H. A. Finlayson, P. Flicek, et al. 2020. An improved pig reference genome sequence to enable pig genetics and genomics research. *GigaScience*. 9:giaa051. doi:10.1093/gigascience/giaa051.

Woodward, A. M., S. Lehoux, F. Mantelli, A. Di Zazzo, I. Brockhausen, S. Bonini, and P. Argüeso. 2019. Inflammatory stress causes N-glycan processing deficiency in ocular autoimmune disease. *Am. J. Pathol*. 189:283–294. doi:10.1016/j.ajpath.2018.10.012.

Xie, Y., Z. Liu, J. Guo, X. Su, C. Zhao, C. Zhang, Q. Qin, D. Dai, Y. Zhao, Z. Wang, et al. 2021. MicroRNA-mRNA regulatory networking fine-tunes polyunsaturated fatty acid synthesis and metabolism in the inner Mongolia Cashmere goat. *Front. Genet*. 12:649015. doi:10.3389/fgene.2021.649015.

Xing, K., H. Liu, F. Zhang, Y. Liu, Y. Shi, X. Ding, and C. Wang. 2021. Identification of key genes affecting porcine fat deposition based on co-expression network analysis of weighted genes. *J. Anim. Sci. Biotechnol*. 12:100. doi:10.1186/s40104-021-00616-9.

Yang, X., L. Li, X. Chai, and J. Liu. 2022. The association between ST8SIA2 gene and behavioral phenotypes in children with autism spectrum disorder. *Front. Behav. Neurosci*. 16:929878. doi:10.3389/fnbeh.2022.929878.

Youn, K., S. Lee, and M. Jun. 2018. Gamma-linolenic acid ameliorates Aβ-induced neuroinflammation through NF-κB and MAPK signalling pathways. *J. Funct. Foods*. 42:30–37. doi:10.1016/j.jff.2017.12.065.

Zeibig, S., M. Büttcher, S. Goebel, J. Pauli, A. Hunger, M. Ungerer, M. Gawaz, and G. Münch. 2019. The scavenger receptor CD68 regulates platelet mediated oxidized low-density lipoprotein (oxLDL) deposition in atherosclerotic vessels at an early stage of atherosclerosis in LDLR−/−/ApoBec−/− mice. *Cell. Physiol. Biochem*. 52:681–695. doi:10.33594/000000048.

Zhang, Z., Z. Yao, and R. Zhang. 2018. Noncoding RNA-targeted therapeutics in autoimmune diseases: from bench to bedside. In: Zhang, R., editor. *The epigenetics of autoimmunity*. Cambridge, MA: Academic Press; p. 359–386.

Zhang, Y., Y. Yu, X. Su, and Y. Lu. 2021. HOXD8 inhibits the proliferation and migration of triple-negative breast cancer cells and induces apoptosis in them through regulation of AKT/mTOR pathway. *Reprod. Biol*. 21:100544. doi:10.1016/j.repbio.2021.100544.

Zheng, Z., Y. Ge, J. Zhang, M. Xue, Q. Li, D. Lin, and W. Ma. 2015. PUFA diets alter the microRNA expression profiles in an inflammation rat model. *Mol. Med. Rep*. 11:4149–4157. doi:10.3892/mmr.2015.3318.

Zivkovic, A. M., N. Telis, J. B. German, and B. D. Hammock. 2011. Dietary omega-3 fatty acids aid in the modulation of inflammation and metabolic health. *Calif. Agric*. 65:106–111. doi:10.3733/ca.v065n03p106.